Journal of Electronic Materials (2022) 51:1568–1582
https://doi.org/10.1007/s11664-021-09390-w

ORIGINAL RESEARCH ARTICLE

In situ TEM Characterization of Phase Transformations and Kirkendall Void Formation During Annealing of a Cu–Au–Sn–Cu Diffusion Bonding Joint

L. Cornet[1] · L. Yedra[1] · É. Héripré[1] · V. Aubin[1] · J.-H. Schmitt[1] · M.-L. Giorgi[1,2]

Received: 6 May 2021 / Accepted: 6 December 2021 / Published online: 18 January 2022

Abstract
Diffusion bonding with Au, Cu and Sn is a technique that can be used to manufacture printed circuit boards. The mechanisms of reactive diffusion and Kirkendall void formation were studied in the Cu–Au–Sn–Cu sandwich system. The initial thickness of the Au and Sn layers was a few micrometers, corresponding to 57 mol.% Au and 43 mol.% Sn. The experiments were conducted *in situ* in a transmission electron microscope (TEM). The TEM thin diffusion couple was heated to 240°C at a rate of 6.5°C/min and then held at 240°C for approximately 2 h. The Au-Sn interaction and progressive enrichment in Cu induce the nucleation and growth of different phases. After heating to 230°C, only binary intermetallic compounds are formed. Between 230°C and 240°C, the ternary phase B develops, replacing the other phases. Over longer periods at 240°C, phase B is progressively consumed on each interface with Cu and replaced with $AuCu_3$. The diffusion path theory is used in the ternary Au-Cu-Sn diagram to analyze the chemical evolution of the system and the flux of elements through the interfaces. The nucleation and growth of Kirkendall voids are observed in parallel with reactive diffusion at both interfaces. The formation of Kirkendall voids appears to be primarily related to the growth of phase B. Mechanisms based on different diffusion rates for the elements are proposed to explain the formation of these voids.

Keywords Au–Cu–Sn system · intermetallic compounds · reactive diffusion · growth · voids evolution

Introduction

Diffusion bonding is an assembly technique that is widely used in advanced industries such as aerospace, aeronautics, automotive and microelectronics. This technique is of particular interest for the printed circuit boards (PCB) industry to produce interconnects in a multilayer printed circuit. This allows the manufacturing of cost-effective and highly complex 3D structures which allow one, for instance,[1]

- To perform internal connections without drilling a hole through the entire stack (facilitate design by reducing the number and diameter of holes),
- To manufacture and assemble several simple PCB to form complexes circuits, reducing the cost of waste, and
- To extend the maximal thickness and number of layers of the PCB.

The elements to be connected must be covered with a layer of copper. Each interface to bond is then covered with a different metal .[1] The elementary printed circuits are stack together under a few tens of bars, and the assembly is heated at a temperature of about 200°C to end up with diffusion at the solid-state and the formation of a joint within the metallic parts. An arrangement in which one Cu layer is coated with Au while the other is coated with Sn, both at the micrometer scale, has shown promising results.[1]

This paper focused on an industrial Cu/Au/Sn/Cu succession of layers when bonded at 240°C. Most of the studies concerning diffusion in the Au-Cu-Sn ternary system have focused on interfacial reactions in diffusion couples in the

✉ L. Cornet
louis.cornet@centralesupelec.fr

✉ V. Aubin
veronique.aubin@centralesupelec.fr

[1] LMPS, Université Paris-Saclay, ENS Paris-Saclay, CentraleSupélec, CNRS, 91190 Gif-sur-Yvette, France

[2] LGPM, CentraleSupélec, Université Paris Saclay, 3 rue Joliot-Curie, 91192 Gif-sur-Yvette cedex, France

solid-state (Au–29 mol.% Sn/Cu,[2,3] Sn–0.3 to 0.7 wt.% Cu/Au,[4] Au–20 to 80 mol.% Cu/Sn[5,6]) where the initial couple can be considered semi-infinite or in liquid/solid reactions (Au–29 mol.% Sn/Cu[2,7,8]). A limited number of studies have been carried out on microstructure evolution in sandwich samples (Cu/Au–29 mol.% Sn/Cu,[2] Au/Sn/Cu,[9] Sn/Au/Cu[8]). To our knowledge, no studies have been carried out on Cu/Au/Sn/Cu samples during solid-state diffusion with Au and Sn layer thicknesses of only a few micrometers between two thick copper strips. During their lifetime, such multilayered printed circuits must endure vibrations and thermal cycles. Beyond the electrical properties, it is then of primary importance to optimize the microstructure of the bond in order to provide a high mechanical resistance to avoid any failure which could be detrimental. Among the microstructural parameters, the presence of voids and porosity, such as Kirkedall voids, in the bond strongly affect its mechanical resistance. The microstructure and damage evolve during the solid diffusion process and a better understanding of their evolution with the process parameters leads to a general improvement of the multilayered printed circuit.

Previous studies[2–10] show that the initial layers of the system are consumed to form the reaction products and may even be consumed entirely in some cases. Diffusion of the elements is accompanied by the creation of intermetallic compounds (IMCs) found in the Au-Cu-Sn ternary system.[11,12] The typical microstructure obtained is composed of a succession of planar layers of IMCs such as Cu_3Sn, $AuCu_3$, $(Cu, Au)_6Sn_5$ and the ternary B phase (20 mol.% Sn, from 45 to 60 mol.% Cu, balanced Au), which is present in almost all of the studies.[3,5–7,10] The other two ternary IMCs,[11] noted A (20 mol.% Sn, from 33 to 36 mol.% Cu, balanced Au) and C (32 mol.% Sn, ~30 mol.% Cu, balanced Au), are mentioned only once.[7] Of course, the initial configuration and temperature (150 to 360°C) of the system have a significant impact on the microstructure and its evolution.

It is well known that differences in atom diffusion fluxes lead to a flux of vacancies, which can coalesce and form pores called Kirkendall voids.[13] The formation of Kirkendall voids has been reported in binary Cu/Sn and Au/Cu diffusion couples.[14,15] Recent studies have shown that the electroplating process for depositing thin layers of Cu and Au has a significant impact on pore formation when large quantities are involved.[16–19] Since the reliability of the joints decreases in the presence of Kirkendall voids,[20,21] it is essential to gain a better understanding of void formation. However, there are no experimental data on Kirkendall voids for ternary Au-Cu-Sn systems. We, therefore, propose to study them using *in situ* transmission electron microscopy (TEM).

The use of *in situ* TEM experiments to study diffusion-induced phase formation and transformation is a recent development.[22–24] For the system of interest, Kotula and Prasad[25] studied the formation of Kirkendall voids in the Cu/Au diffusion couple by conducting an *in situ* TEM heating experiment. They demonstrated that columnar grain boundaries in Au coatings were fast diffusion pathways for Cu. The different diffusion rates of Cu and Au resulted in the formation of Kirkendall voids in Cu.

In summary, the present study aims to examine the mechanisms of reactive diffusion and Kirkendall void formation in the Cu-Au-Sn-Cu sandwich system. The experiments were conducted on diffusion couples heated *in situ* in the TEM to identify the fundamental diffusion mechanisms directly as they occur. To our knowledge, such a study has never been reported in the open literature for the Cu-Au-Sn-Cu system. The approach used is as follows:

(1) A thin Cu/Au/Sn/Cu sample is annealed at 240°C for 2 h *in situ* in the TEM.
(2) *in situ* observations allow the formation of voids to be visualized. Analyses using energy-dispersive x-ray spectroscopy (EDS) were performed at various points during the heat treatment, after cooling to room temperature, to determine the phases present.
(3) Reaction and pore formation mechanisms are proposed based on the interpretation of the observations made in conjunction with the chemical analyses performed.

Experimental Techniques

The experimental protocol aims to produce a thin Cu–Au–Sn–Cu diffusion couple and to observe its transformation when heated to 240°C in a transmission electron microscope (TEM). TEM sample preparation, diffusion experiments and the characterization procedure are described in Materials and TEM Sample Preparation and Diffusion Experiments and Characterization sections, respectively.

Materials and TEM Sample Preparation

Elvia PCB Group supplied Cu specimens coated with Sn and Au. The preparation starts with two sets of 30-µm-thick cold-rolled Cu strips, electroplated with 10 µm of Cu (Cupracid TP1). The first set of Cu strips was then coated on both sides with an approx. 2–3-µm tin layer using the NTS UNISTAN chemical process, while the second set was electroplated on both sides with a 1.5-µm Au layer (AURUNA 550). The exact mean Sn and Au composition in the joint is determined by a material balance based on the joint analysis to account for the thickness variabilities related to the deposition processes (Variations in Mean Joint Composition section).

Square specimens measuring 10 x 10 mm^2 were cut from these strips and stacked alternately to produce a sequence of ten Cu–Au–Sn–Cu diffusion couples. These stacks were

then placed in a homemade pressure device to ensure good contact between the diffusion couple surfaces.

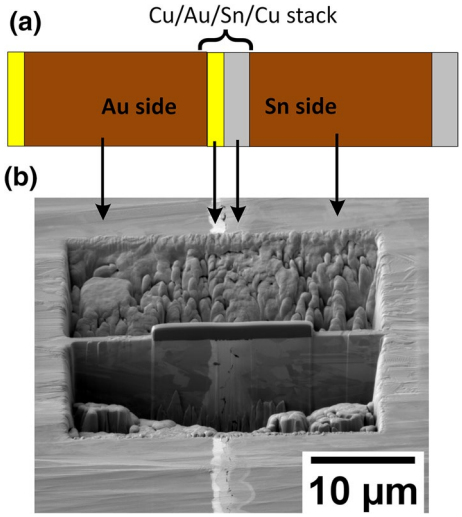

Fig. 1 (a) Schematic representation of the initial stack with Cu in brown, Au in yellow and Sn in grey, (b) FIB image showing the selected joint and the TEM thin foil extracted perpendicularly to this joint.

The stacks were placed in a furnace preheated to 50°C. They were heated to 230°C at a rate of 6.5°C/min then water-quenched to preserve the high-temperature microstructure. By this step, the diffusion process had advanced sufficiently to bond all the diffusion couples together. The top surface of the assembly was then mechanically polished with SiC and mirror-polished with a 3-µm diamond suspension. An area of interest was selected by observation in a focused ion beam (FIB) scanning electron microscope (SEM) (dual-beam SEM FIB HELIOS *FEI NanoLab 660)* (Fig. 1). A 200-nm-thick TEM thin foil was processed using the FIB and extracted in this area perpendicular to the joint (Fig. 1b).

Diffusion Experiments and Characterization

The experimental protocol is described in Fig. 2, including preliminary heating of the bulk specimen and lamellae extraction (Materials and TEM Sample Preparation section), followed by a thermal cycle and EDS analysis performed on the FIB foil.

The thin foil was soldered onto FUSION E-chips (Protochips) and placed in a probe Cs-corrected scanning transmission electron microscope (TEM/STEM TITAN-FEI *Titan3 G2 60-300)* for the *in situ* thermal cycle. Before heating, dark field images and analyses were performed

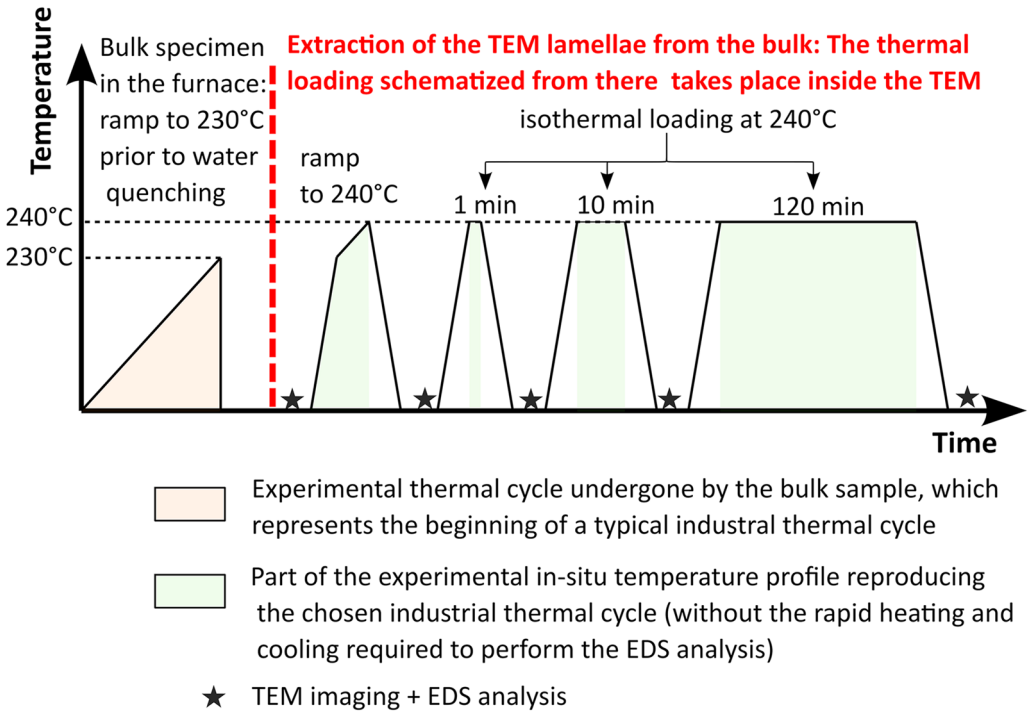

Fig. 2 Schematic illustration of the thermal cycle applied to the sample. The first step consists of heating the bulk sample to 230°C at a rate of 6.5°C/min to obtain the adhesion of the Cu/Au/Sn/Cu diffusion couple (part shaded in orange). A TEM sample can then be extracted from the bulk sample and placed in the TEM. The thermal cycle undergone by the TEM sample (end of heating at 6.5°C/min from 230°C to 240°C and holding at 240°C for 131 min) reproduces a typical industrial thermal cycle (parts shaded in light green). Additional high-rate heating and cooling are required for EDS analyses and TEM images (Color figure online).

using energy dispersive spectroscopy (4-detector Super-X EDS) at 300 kV to determine the initial state of the diffusion couple. Diffusion starts during heating and a first reaction is needed between Au and Sn layers to join the two sides of the diffusion couple. This step is required to be able to easily machine a TEM thin foil normal to the joint. Previous trials have shown that, for a 6.5°C/min heating ramp, 230°C represents an adequate temperature which gives rise to a reference microstructure, which allows *in situ* study of the last part of heating to and holding at 240°C.

The thermal cycle used was chosen in order to reproduce an industrial diffusion bonding process consisting of heating at a rate of 6.5°C/min and holding at 240°C for 120 min. This thermal loading is representative of diffusion bonding in the PCB industry.[1] As described in Materials and TEM Sample Preparation section, the TEM sample was extracted from a bulk specimen heated to 230°C, which corresponds to the initial state of the *in situ* experiment. For this reason, the TEM sample was heated to 230°C at a rapid rate of 120°C/min, and the foreseen thermal cycle was then continued with the heating ramp to 240°C at 6.5°C/min followed by holding at 240°C for 131 min. The diffusion and phase transformation taking place during the second heating stage from room temperature to 230°C are negligible because of the rapid heating rate.

Images were acquired continuously in scanning mode (STEM) for the duration of the *in situ* experiment, with an acquisition rate of 2 Hz at the beginning of the experiment (up to 1min at 240°C), then 1 Hz (during the 10 min at 240°C) and finally one frame per minute. The acquisition rate is decreased because the microstructure changes become slower and slower as the annealing time increases. The chemical composition was characterized by EDS analysis at various times after 240°C had been reached (0, 1, 10, and 120 min). Since this type of measurement takes about 30 min to obtain quantitative element maps, the sample was cooled down to room temperature at a rate of 430°C/min prior to EDS analysis and then heated to 240°C after analysis, to maintain the microstructure unchanged during analysis.

In short, the thin foil undergoes four cycles of heating at 120°C/min, slower heating at 6.5°C/min or holding at 240°C, cooling at 430°C/min, and analysis (Fig. 2). The intermediate heating and cooling phases are very fast (120°C/min and 430°C/min respectively).

During heat treatment, void formation was observed. The area and number of these voids were quantified by image analysis using ImageJ software[26,27]: a binarization was applied to all of the images taken during the *in situ* experiment to differentiate voids (white) from matter (black). A conventional particle analysis was then performed with a minimum surface area of 0.01 μm^2 to avoid noise.

For each EDS analysis, a complete mapping of the joint reaction zone was carried out. The EDS spectra were processed quantitatively with the ESPRIT 1.9 (Brucker) software using the Cliff-Lorimer method, which is suitable for quantitative analysis on thin samples. Large areas within each layer were extracted from the element maps to measure the average and the standard deviation of the composition of the different phases. Composition profiles perpendicular to the joint, also extracted from the element maps, were used to observe the composition gradients of the joints. The composition profiles are the average of ten profiles, to reduce the EDS measurement noise. Image processing was also performed to remove the quantification artefact of the EDS analysis in the voids, where composition must be zero.

Experimental Results

Initial State: Microstructure at 230°C

The sample was observed after initial heating to 230°C and before *in situ* annealing in the TEM (Materials and TEM Sample Preparation and Diffusion Experiments and Characterization sections). First of all, a dark field (DF) image gives an overview of the thin foil (Fig. 3a). The left side of the sample corresponds to the gold deposition side (later referred to as the Au-rich side), while the right side is related to the tin deposition side (Sn-rich side). This reference will be kept constant throughout the presentation of the results. The interfaces appear to be less rough on the Au-rich side than on the Sn-rich side, probably due to the early stages of reactive diffusion below 230°C, which differ from one side to the other.

The heating rate is such that diffusion already occurs during the temperature increase, creating a bond between the two sides of the diffusion couple. This part of the protocol is necessary for machining the thin TEM sample. A few cracks remain along the contact surface (black lines between layers 2 and 3 in Fig. 3a), probably due to insufficient pressure on the stack. Nevertheless, more than half of the contact surface looks good and, as shown below, the diffusion process can take place under good conditions between the two sides of the diffusion couple.

EDS composition maps reveal that the microstructure of the joint is composed of a succession of four clearly defined layers, numbered 1 to 4 in Fig. 3a, with little variation in thickness (Table I). The chemical composition of each layer is almost constant (Fig. 3e). The quantitative analysis of their composition is presented in Table I. Layers 1 and 4 are composed of the intermetallic compounds Au_3Cu and Cu_3Sn, respectively. The mean composition of layer 3 is close to

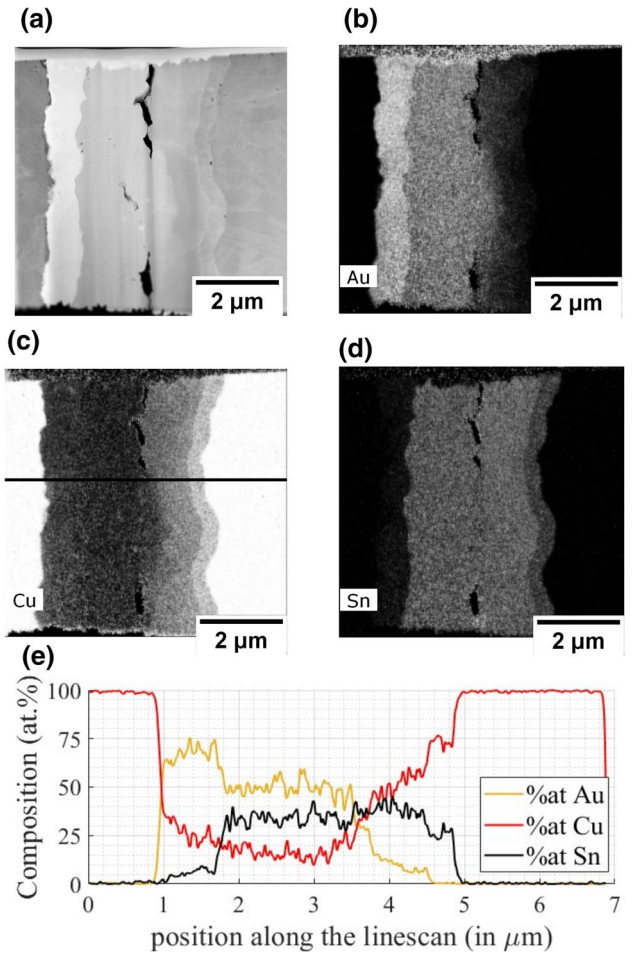

Fig. 3 (a) Dark-field images and EDS mapping of (b) Au (c) Cu and (d) Sn after initial heating to 230°C and before *in situ* annealing in the TEM. The composition of the elements increases as the grey levels change from black to dark grey, light grey, and white. The horizontal black line in the Cu mapping (c) indicates the position of the linescan presented in (e). The composition of Au, Cu and Sn in each layer is homogeneous

Table I Average and standard deviation of Au, Cu and Sn composition and average thickness of the four layers highlighted by the EDS analysis presented in Fig. 3. The corresponding possible phases are given in the last row

Layer number in Fig. 3a	1	2	3	4
Composition mol.% Cu	23 ± 3	17 ± 3	50 ± 4	75 ± 2
Composition mol.% Au	71 ± 5	50 ± 3	12 ± 3	1.0 ± 0.1
Composition mol.% Sn	5 ± 1	34 ± 1	40 ± 1	24 ± 2
Thickness (µm)	0.7 ± 0.1	1.7 ± 0.3	1.0 ± 0.2	0.4 ± 0.1
Possible phase	Au_3Cu	(Au,Cu)Sn	$(Cu,Au)_6Sn_5$	Cu_3Sn

the binary compound Cu_6Sn_5 with Au in substitution. It can be assumed that layer 3 is composed of $(Cu, Au)_6Sn_5$, even though it is slightly depleted in Sn (40 mol.% instead of 45 mol.%). The mean composition of layer 2, positioned in the Au-Cu-Sn ternary diagram at 240°C[11] (Fig. 9), is located in the two-phase domain between AuSn and phase A. If the system were in equilibrium, layer 2 would therefore be composed of phase A and AuSn. However, the composition of layer 2 is homogeneous (Fig. 3e), which suggests that it consists of a single phase. This metastable phase could be (Au, Cu)Sn slightly depleted in Sn. To go further, electron diffraction would have to be performed on a thinner TEM foil than the one used in the heating tests presented here. This is beyond the scope of the study.

Assuming that the cracks in the middle of the TEM foil correspond to the initial Au/Sn interface, it can be said that Au diffusion is low on the Sn-rich side. Indeed, about 12 mol.% Au is found in layer 3 to the right of the cracks. Conversely, Sn is more homogeneously distributed within the joint as a whole (layers 2 and 3 containing 34 mol.% to 40 mol.% Sn), other than in a thin layer along the initial Cu/Au interface where Sn is only slightly present (5 mol.%).

The melting temperature of Sn is 231°C, but after the first temperature rise to 230°C the Sn reacted to form intermetallic compounds, which have melting temperatures higher than 231°C. The joint is hence expected to be unable to undergo the transition to the liquid state upon subsequent annealing.

Microstructure Evolution During *in situ* Heating and Holding

The initial well-characterized joint is then heated to 240°C and maintained at this temperature *in situ* in the TEM (Fig. 2).

Figure 4 shows the high-angle annular dark-field (HAADF) images as well as the EDS maps of Au, Cu, and Sn during heating from room temperature to 240°C (Fig. 4a) and after holding at 240°C for 1 min (Fig. 4b), 11 min (Fig. 4c) and 131 min (Fig. 4d). Between the different results presented, it should be recalled that the sample is cooled down to room temperature to allow the EDS measurement (Fig. 2). Additional chemical analyses, corresponding to the horizontal black lines in Fig. 4, are given in Supplementary Material A Fig. S1 to show that the chemical composition of each layer is almost constant. Their mean composition is shown in Table II. The film of the *in situ* evolution of the thin sample can be found in Supplementary Material B (direct STEM acquisition with synchronization of thermal loading). *in situ* observation evidences the appearance of voids (in black in Fig. 4) that accompany the microstructural evolution of the joint at 240°C. These voids will be described in detail in Sect. 3.3. In this section, we focus on phase evolution within the diffusion couple.

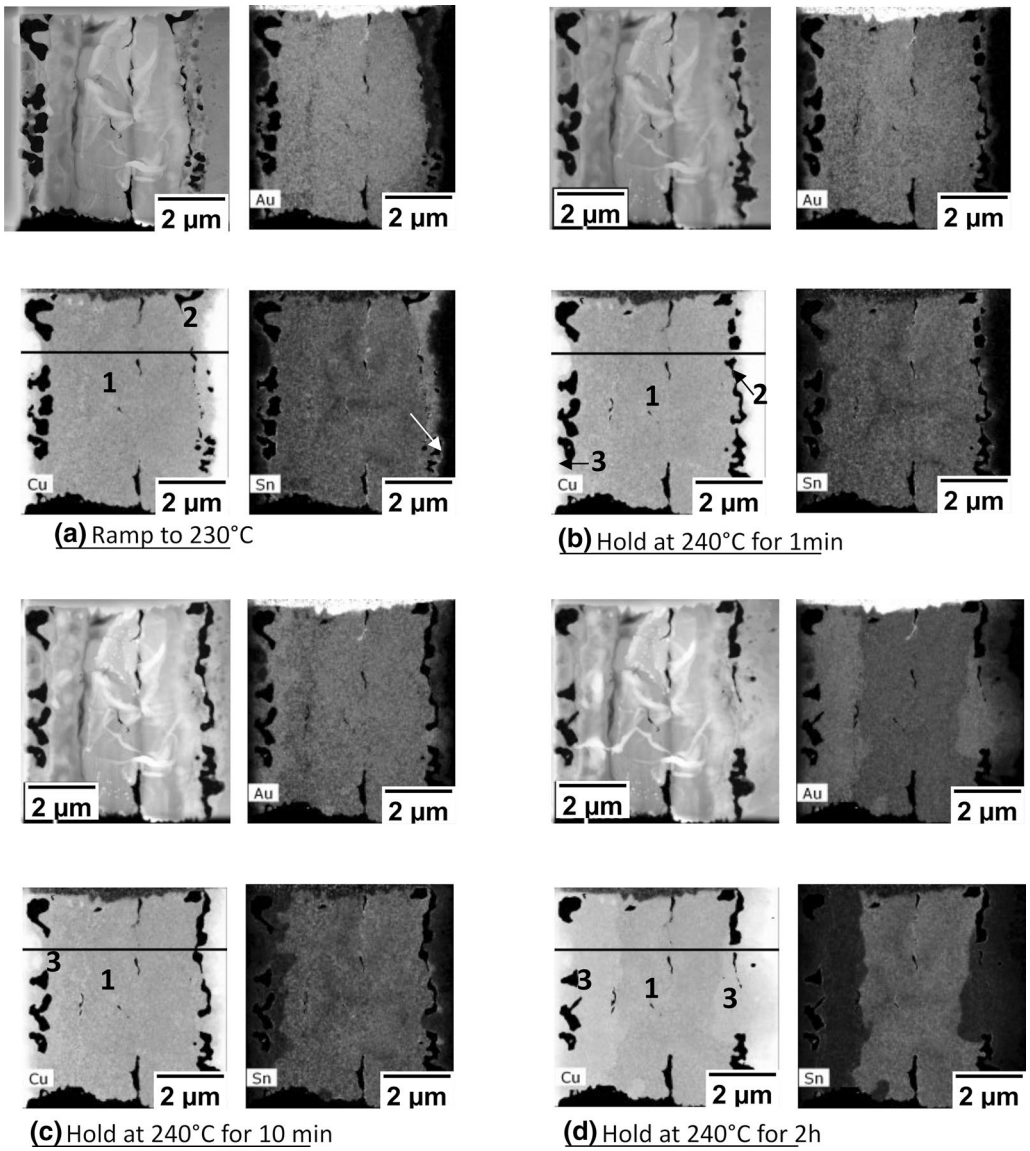

Fig. 4 HAADF images (top left) and EDS maps (Au top right, Cu bottom left and Sn bottom right) performed at the end of each step at 240°C: (a) after reaching 240°C and after a holding time of (b) 1 min, (c) 11 min, and (d) 131 min. The analyses show the evolution of the phases present (1: phase B, 2: Cu_3Sn, 3: $AuCu_3$). The black parts visible at the two-phase interfaces with Cu are holes. The horizontal black line in the Cu maps indicates the position of the linescans presented in Supplementary Material A Fig. S1.

The composition of the elements becomes more homogeneous in most of the joints (zone 1, Fig. 4a and Supplementary Material A) when they are heated from 230 to 240°C. Partial reactions can occur at temperatures below 230°C during the heating step, although a high heating rate of 120°C/min has been chosen to minimize this contribution. The quantitative EDS analysis shows that the joint is formed mainly of a ternary compound, which can be attributed to the phase B reported in the literature[5,11] even if it contains less Sn than in previous studies (around 15 mol.% instead of 20 mol.%) (Table II). This phase appears as a transformation of the first three layers (1, 2, and 3 in Fig. 3a) observed at 230°C through a homogenization of the Au and Sn amounts with significant enrichment in Cu (Tables I and II). A thin layer of Cu_3Sn remains present along the initial Sn/Cu interface (layer 2, Fig. 4a). Its thickness has varied little, and its Au content has increased slightly from 1 to 4 mol.% (Tables I and II). No Au-rich intermetallic compounds were found at the initial Cu/Au interface (left).

After 1 min at 240°C, only a very thin discontinuous layer of Cu_3Sn remains (layer 2, Fig. 4b). On the Au-rich side, a new Sn-free phase appears locally (zone 3, Fig. 4b). These two phases are too small to perform a quantitative EDS analysis, but they are probably Cu_3Sn (detected at the beginning

Table II Mean composition of Au, Cu and Sn and average thickness of the three layers highlighted by the EDS analysis presented in Fig. 4 for all annealing times at 240°C studied (0, 1, 11 and 131 min). NQ (not quantified) indicates that the phase exists but the volume it occupies is too small to allow precise quantification by EDS, and n.d. (not detected) means that the phase does not exist

Annealing time at 240°C (min)	Layer number in Fig. 4	1	2	3
	Possible Phase	Phase B	Cu_3Sn	$AuCu_3$
0	Composition mol.% Cu	60 ± 3	75 ± 3	n.d.
	Composition mol.% Au	24 ± 2	4 ± 1	n.d.
	Composition mol.% Sn	15 ± 1	22 ± 2	n.d.
	Thickness (μm)	4.3 ± 0.3	0.4 ± 0.2	–
1	Composition mol.% Cu	65 ± 2	NQ	NQ
	Composition mol.% Au	20 ± 3	NQ	NQ
	Composition mol.% Sn	15 ± 1	NQ	NQ
	Thickness (μm)	4.4 ± 0.3	–	–
11	Composition mol.% Cu	66 ± 2	n.d.	74 ± 3
	Composition mol.% Au	19 ± 1	n.d.	20 ± 3
	Composition mol.% Sn	15 ± 1	n.d.	6 ± 1
	Thickness (μm)	4 ± 0.2	–	0.5 ± 0.2
131	Composition mol.% Cu	70 ± 1	n.d.	77 ± 1
	Composition mol.% Au	14 ± 1	n.d.	18 ± 1
	Composition mol.% Sn	16 ± 1	n.d.	5.0 ± 0.3
	Thickness (μm)	3.2±0.3	–	1.4 ± 0.5 0.6 ± 0.5

of the heat treatment at 240°C, Fig. 4a) and $AuCu_3$ (detected over longer periods, Figs. 4c and 4d). Phase B constitutes the vast majority of the joint; its chemical composition has been depleted in Au by nearly 4 mol.% and enriched in Cu by 5 mol.% (Table II).

After 11 min at 240°C, the joint still consists mainly of phase B (zone 1, Fig. 4c). On the Au-rich side between Cu and phase B (zone 3, Fig. 4.c), the phase detected previously is now clearly visible. The EDS analysis indicates a composition close to $AuCu_3$, with a small amount of Sn. On the other side of the joint, the Cu_3Sn layer has disappeared completely or, at least, become so thin that it is no longer visible. On the same side, small areas of $AuCu_3$ are detected but do not yet form a continuous layer.

At the end of the *in situ* experiment, an $AuCu_3$ layer has developed on both sides. The thicker layer is on the Au-rich side (1.4 μm). It is the result of a decrease in Au content of 5 mol. % in phase B, while the amount of Cu increases by 4 mol.% (Table II). On the Sn-rich side, irregular growth of $AuCu_3$ is observed along the interface between the voids (zone 3 on the right side of Fig. 4d).

Evolution of the Kirkendall Voids

in situ observations revealed voids that appear black in Fig. 4 when the thin sample is heated to 240°C. We will now describe these voids, which are due to the Kirkendall effect as explained below, in greater detail.

No voids were observed after initial heating to 230°C in the bulk sample (Fig. 3). This means that Kirkendall voids are initiated and developed later in the temperature ramp from 230°C to 240°C and mainly during annealing at 240°C. These voids appear at the Cu/Au interface on the left and the Sn/Cu interface on the right. Figures. 5 and 6 show the variations in their number and the surface area they occupied as a function of the annealing time (up to 20 min in Fig. 5 and more than 20 min in Fig. 6). A reminder of the temperature profile is given at the top of Figs. 5 and 6. The annealing time corresponds to the cumulative time during which the thin sample undergoes a temperature profile (heating, holding and cooling). The time required for EDS measurements at room temperature is not counted in this time. Cooling to room temperature has no influence on the formation and evolution of Kirkendall voids at temperatures below 230°C, which means that reactive diffusion is negligible during these periods. Dark-field images corresponding to four key annealing times at the start of annealing at 240°C are shown, focusing on the voids (Fig. 5d).

A distinction is made between the initial Cu/Au and Sn/Cu interfaces shown in the figures and below because the Kirkendall voids grow in different ways at the two interfaces.

Au-Rich Side

At the Cu/Au interface, the voids are all formed at the end of the first temperature increase to 240°C (~ 5 min in Fig. 5). During this time, the surface area occupied by the voids increases and reaches a maximum. Kirkendall voids are characterized by a low density of nucleation sites and a growth rate of about 1.2 $\mu m^2 min^{-1}$ with a mean variation in radius of 0.1 μm min^{-1}. The growth occurs without preferential orientation, resulting in a few large, almost equiaxed voids. After heating to 240°C, the voids are observed to be in phase B at the Cu/phase B interface. With this experiment, it is not possible to locate exactly where the voids are nucleated because this position within the phases present can only be determined with EDS analyses. The voids have

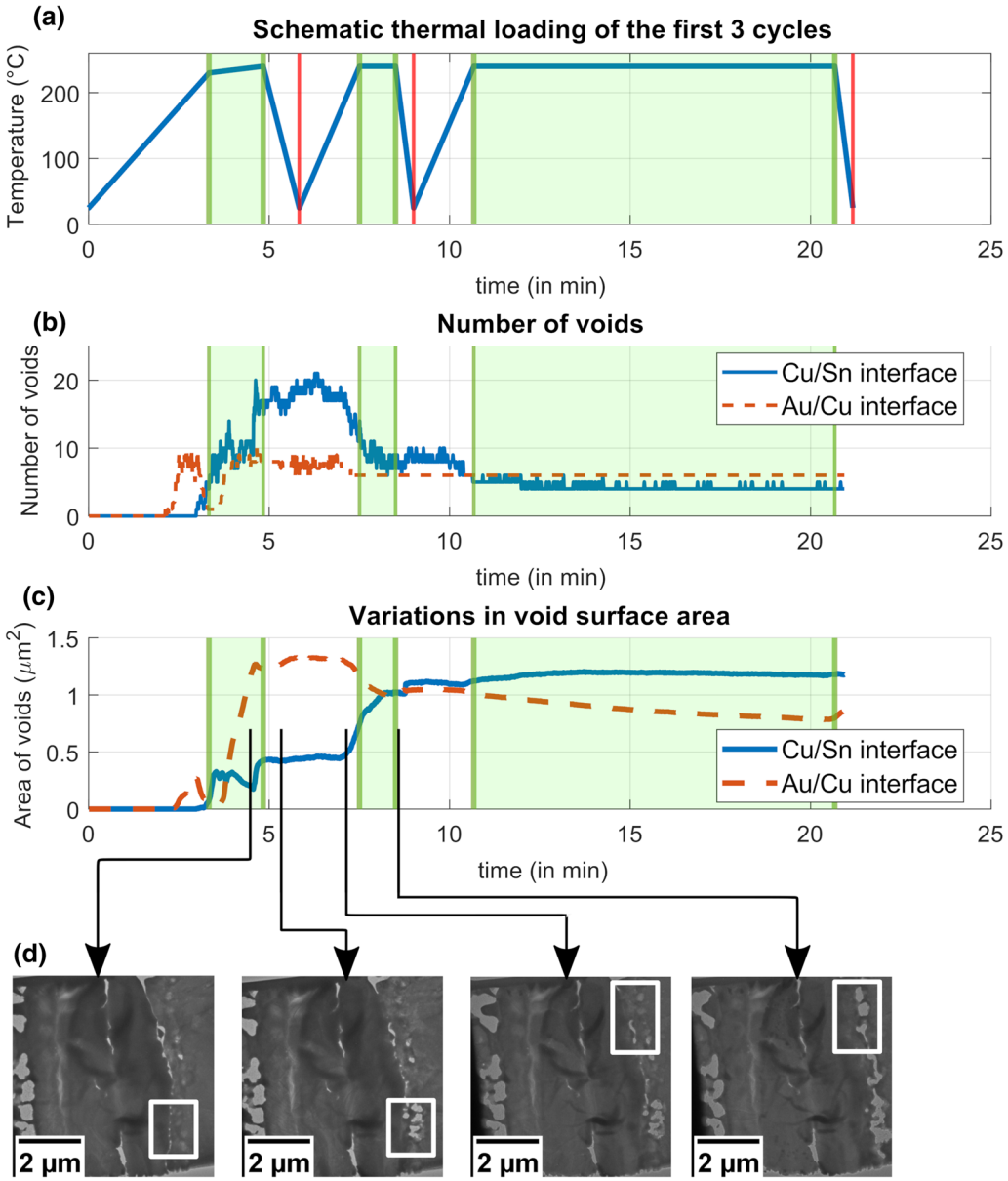

Fig. 5 Evolution of Kirkendall voids in the thin Cu/Au/Sn/Cu sample as a function of the temperature profile (a) for times shorter than 20 min, with (b) the number of voids, (c) the area occupied by these voids and (d) dark-field images corresponding to key annealing times at 240°C. The surface area of the voids increases faster on the Cu/Au side (left) than on the Sn/Cu side (right). There are fewer voids on the Cu/Au side than on the Sn/Cu side for the first 10 min of heat treatment. Subsequently, the number of voids on both sides becomes comparable.

already formed when the second EDS analysis is performed after the first holding at 240°C.

During the subsequent heat treatment, the number of Kirkendall voids remains almost constant and their surface area decreases slowly, with slower and slower kinetics, i.e. 0.022 μm^2/min before 11 min (Fig. 5) and 0.002 μm^2/min thereafter (Fig. 6). The positions of the voids remain unchanged: embedded in the joint, in the newly formed Au_3Cu, at the interface with Cu.

Sn-Rich Side

The evolution of the voids is more complex on the Sn-rich side.

The first step of void nucleation occurs at 230°C at the phase B/Cu_3Sn interface. The voids expand rapidly (1.4 μm^2/min) along this interface, forming an almost continuous thin crack. When the temperature increases to 240°C, the thickness of this crack decreases and the voids form a dotted

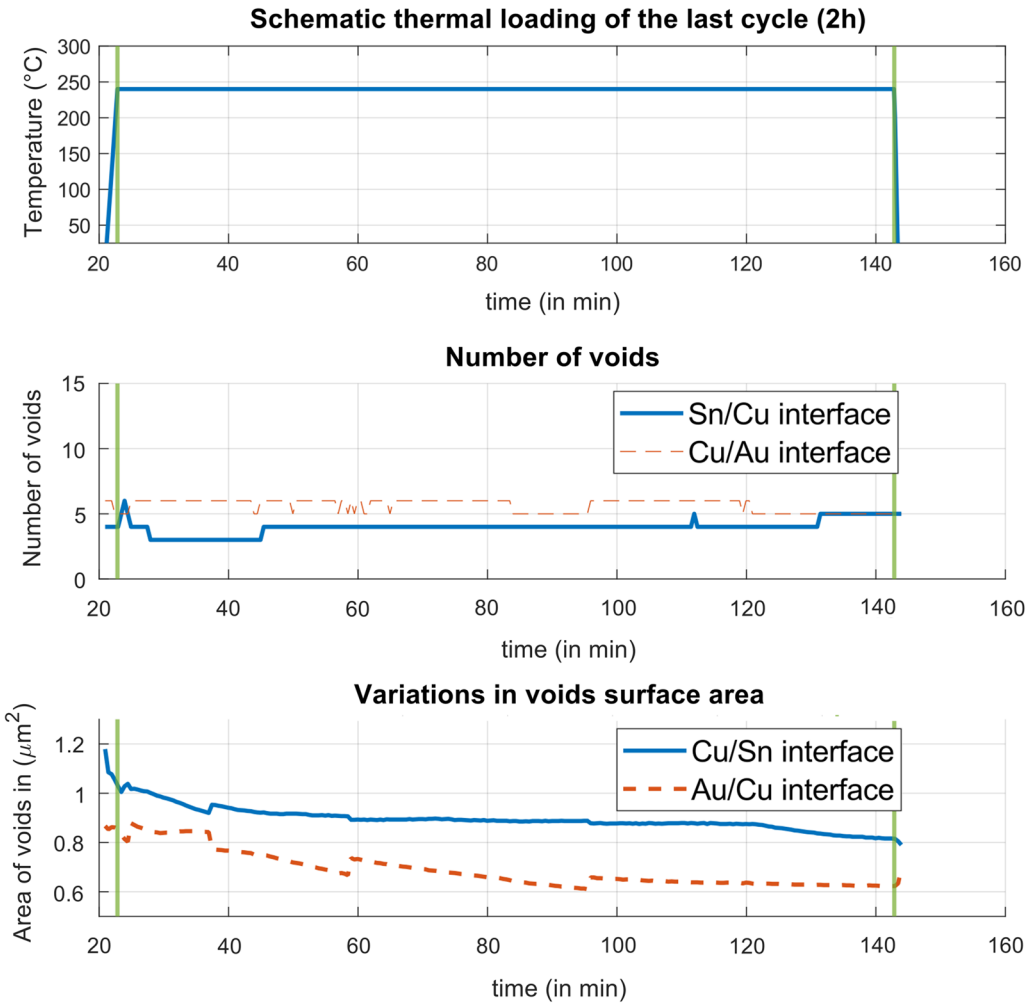

Fig. 6 Evolution of Kirkendall voids in the thin Cu/Au/Sn/Cu sample as a function of the temperature profile (a) for times longer than 20 min, with (b) the number of voids and (c) the area occupied by these voids. The surface area of the voids decreases slowly while the number of voids remains constant.

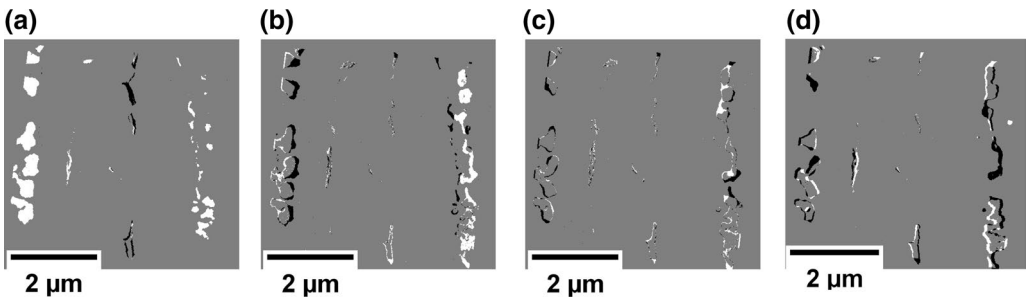

Fig. 7 Evolution of the voids in the thin sample during heat treatment (a) from 230 to 240°C and at 240°C, (b) between 0 and 1 min, (c) between 1 min and 11 min, and (d) between 11 min to 131 min. A void or alloy present at the same location between two annealing times is light grey. A void that has formed appears white and a void that has been filled appears black.

line along the interface. The number of voids and their surface area remain almost constant for about 1 min. Then new nucleation sites form inside the Cu_3Sn, close to the interface with the Cu, resulting in a large increase in the number of voids and a slight decrease in their surface area. This leads to a change in the location of the voids during subsequent

heating (Fig. 5d), as will also be shown in Sect. Apparent Movement of the Voids at Both Interfaces (Fig. 7) and the *in situ* recordings (see supplementary material B).

During the second heating and holding stage at 240°C, the number of voids decreases and their surface area increases. The density of the nucleation sites is higher than on the Au-rich side, allowing neighbouring voids to coalesce as they grow (white rectangles, Fig. 5d).

During the third holding stage at 240°C, after 4 min at 240°C, a dozen voids coalesce to form a succession of three large voids, covering almost the entire boundary between the joint and the Cu. This gives a maximum void area of 1.2 μm^2, which then remains constant. During the last rise to 240°C (between 11 min and 131 min of annealing), the surface area of the voids decreases from 1.2 to 0.8 μm^2.

Apparent Movement of the Voids at Both Interfaces

Image processing is carried out to track the evolution of the voids (formation and filling) during heat treatment. To do this, the HAADF images shown in Figs. 3 and 4 are binarized and subtracted two by two to capture the changes between 230°C and 240°C (Fig. 7a), at 240°C between 0 and 1 min (Fig. 7b), between 1 min and 11 min (Fig. 7c), and between 11 min and 131 min (Fig. 7d). The colour code for interpreting the results is as follows: a void or alloy present at the same location between two annealing times is light grey. A void that has formed appears white and a void that has been filled appears black.

The cracks initially present in the middle of the diffusion couple (Sect. Initial State: Microstructure at 230°C) are partially closed at the end of the 230–240°C temperature ramp. Numerous voids form at both interfaces: some large ones at the Cu/Au interface and many small ones at the Cu/Sn interface. Between 0 and 1 min at 240°C (Fig. 7b), the voids appear to move towards the outside of the joint (to the left in the case of the Cu/Au interface and to the right in the case of the Sn/Cu interface). As the annealing time lengthens, the voids tend to close.

Discussion

In Sect. Experimental Results we described the transformation of the Cu/Au/Sn/Cu diffusion couple during heating to and holding at 240°C. Because of progressive enrichment in Cu, intermetallic compounds form and disappear in a complex succession. Voids are observed to nucleate and grow in parallel with reactive diffusion. The mean composition of the joint is discussed first (Variations in Mean Joint Composition section). Reaction mechanisms that could explain the transformation of the joint and the formation of Kirkendall voids are then proposed based on the diffusion path theory and flux analysis (Sect. Variations in Joint Microstructure).

Variations in Mean Joint Composition

The mean joint composition was calculated from the EDS element maps at the different annealing stages (230°C; 240°C: 0 min, 1 min, 11 min, and 131 min). The results are shown in Fig. 8 with the grey dots plotted in the Au-Cu-Sn ternary phase diagram at 240°C (according to the assessment in[11]). The ratio of the molar fractions of Sn and Au x_{Sn}/x_{Au} is constant during joint transformation. From these measurements, it is then possible to estimate this ratio at 0.75 ±0.01. The initial joint composition before any reactive diffusion is, therefore, 57 mol.% Au and 43 mol.% Sn in our experiments (solid red circle on the Au-Sn side in the ternary diagram).

As the temperature is increased, the joint is gradually enriched in Cu. Therefore, the mean joint composition

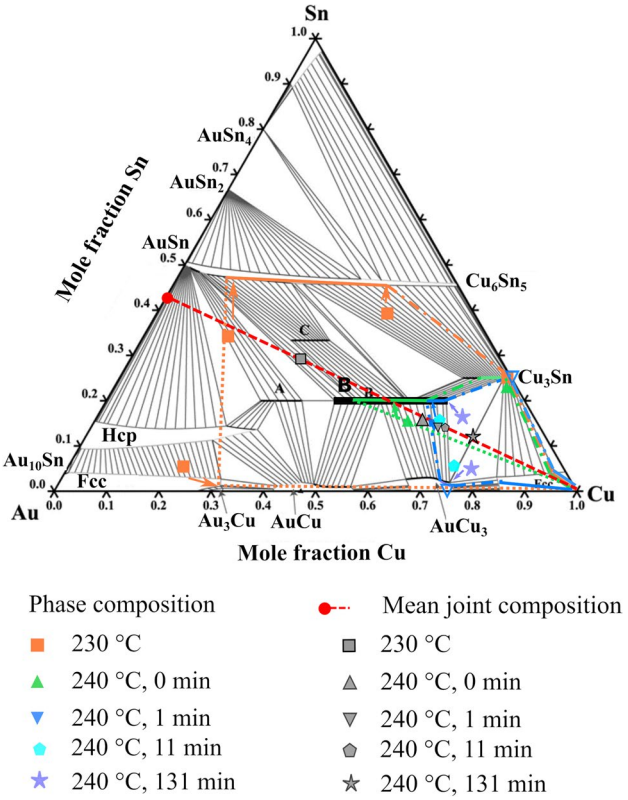

Fig. 8 Variations in joint phase composition at the various annealing stages (230°C ■; 240°C, 0 min ▲, 1 min ▼, 11 min ⬟, and 131 min ★) in the Au-Cu-Sn ternary phase diagram at 240°C [11]. The corresponding mean joint composition is also given (dark grey dots). During annealing the joint is enriched with Cu, which induces nucleation and growth of different phases. The diffusion paths show the resulting microstructures with the interfaces at equilibrium (dashed-dotted lines following the tie lines) or out of equilibrium (dotted lines) (Color figure online).

follows the red dotted line (Fig. 8) from the initial state on the Au-Sn side (solid red circle where Cu has yet to diffuse) to pure Cu (infinite Cu enrichment). The variation in the mean joint composition as a function of annealing time (grey dots) confirms the Cu enrichment and the constancy of the Sn/Au ratio during the diffusion process.

Variations in Joint Microstructure

Figure 8 also shows the variations in joint microstructure at the different annealing stages (230°C; 240°C, 0 min, 1 min, and 131 min) in the Au-Cu-Sn ternary phase diagram at 240°C.[11] Each annealing step represented is associated with a colour, the solid dots corresponding to the composition of the layers analyzed in Sects. Initial State: Microstructure at 230°C and Microstructure Evolution During *in-situ* Heating and Holding. The empty dots correspond to a layer that exists but is too thin to be analyzed accurately (NQ in Table II).

To gain a better understanding of the reaction mechanisms involved, the joint microstructure is visualized with diffusion paths[28,29] in Fig. 8. The diffusion path represents the variations in average composition in planes parallel to the original Cu/joint/Cu interfaces throughout the diffusion zone. The conventions used to draw the diffusion path are consistent with.[28] When two phases are separated by a planar interface in local thermodynamic equilibrium, the diffusion path crosses the single-phase regions (——) and the two-phase region parallel to a tie line (–●–●–). The tie line ends give the composition of the phases in contact at the interface. In the present diffusion system, some phases in contact are not in local thermodynamic equilibrium. In this case, the diffusion path is drawn with a dotted line (●●●●).

Diffusion path theory will be used below to determine whether the interfaces between the phases that form are at local thermodynamic equilibrium and how the joint can evolve during Cu enrichment.

Initial State: Microstructure at 230°C

After heating the bulk diffusion couple to 230°C (orange squares and lines in Fig. 8), the sequence of the reactive layers is as follows: Cu/Au_3Cu/((Au,Cu)Sn/$(Cu,Au)_6Sn_5$/Cu_3Sn/Cu (Sect. Initial State: Microstructure at 230°C). This result is highly consistent with the literature.[11] The intermetallic compounds formed exist in the three binary diagrams, but not all binary compounds are present. This can be explained either by the limited amounts of Sn and Au[30] or by the particular geometry of the thin films, which induce control of nucleation and growth through the kinetics of the interface reactions rather than through solid-state diffusion.[31] In other words, it is not possible to say whether all the binary phases appeared before being consumed by the phases detected at 230°C or whether some phases did not nucleate at all (or are too thin to be observed).

Our measurements show that the composition of the phases detected differs slightly from the compositions indicated in the ternary diagram at 240°C (Fig. 8, orange arrows in the online version). These differences can be explained by analysis uncertainty and by the fact that the joint phases, being continuously enriched in Cu, are not at thermodynamic equilibrium.

The diffusion path at 230°C shows that the phase interfaces on the Sn-rich side are at local thermodynamic equilibrium. Indeed, the Cu/Cu_3Sn and Cu_3Sn/((Cu, Au)$_6Sn_5$ interfaces are represented by the ends of two tie lines. However, on the Au-rich side, thermodynamic equilibrium is not reached at the interfaces (dotted line). In between, the diffusion path crosses the large domain between AuSn and Cu_6Sn_5.[4,32] In the present case, two distinct phases are found (Fig. 3). This result confirms that this large domain could instead be composed of two single-phase regions separated by a two-phase region, as has already been reported.[5,11]

Heating from 230°C to 240°C

As the foil temperature rises from 230°C to 240°C, the joint becomes enriched with Cu from about 30 mol.% (grey square, Fig. 8) to 60 mol.% (grey up-pointing triangle, Fig. 8), causing the Au_3Cu, (Au,Cu)Sn and $(Cu,Au)_6Sn_5$ layers to disappear and phase B to form (Fig. 4a, Table II). At the same time, the Cu_3Sn layer moves to the right, with only a small variation in thickness (Tables I and II). This ternary phase B has been well characterized since the early work of Karlsen et al.[12,33] The reactive diffusion reactions in the thin sample are too fast to reveal the sequence that occurs between 230°C and 240°C. Diffusion pathways and mechanisms are generally accelerated in thin films by several characteristics specific to small systems (high-density grain boundaries, residual stresses) and by the increased contribution of surface atom diffusion (due to the high surface-to-volume ratio for small systems).[25,31] To gain a better understanding of this transformation step, it is necessary to work on bulk samples. This is beyond the scope of the study.

The 240°C diffusion path shows that the phase interfaces on the Sn-rich side have again reached local thermodynamic equilibrium (Fig. 8, green path in the online figure). Indeed, the Cu/Cu_3Sn and Cu_3Sn/B interfaces can be represented by the ends of two tie lines. Thermodynamic equilibrium is not reached at the Cu/phase B interface (dotted line).

The increase in joint thickness, due to the flux of Cu atoms, occurs mainly when the temperature rises from 230°C to 240°C. Indeed, this step corresponds to the highest Cu enrichment in the joint. The position of the central voids does not change during annealing and these can be used as markers to measure interface displacements (Fig. 3a

et 4a). Between 230°C and 240°C, the Au-rich side interface moves towards the copper over about 580±160 nm, while the displacement of the interface on the Sn-rich side is limited to 360±260 nm on average. It can thus be assumed that phase B results from the transformation and mixing of Au_3Cu, (Au,Cu)Sn and $(Cu,Au)_6Sn_5$ induced by the addition of Cu atoms, coming mainly from the Au-rich side and to a lesser extent from the Sn-rich side. Au_3Cu probably disappears quite quickly because phase B is greatly extended on this side. The presence of the Cu_3Sn layer in the Sn-rich side may slow down Cu diffusion and explain the limited Cu flux from this side.

To continue the flux analysis, which is useful for analysing the Kirkendall voids, the variations in the composition of the three elements during annealing measured by EDS can give a good-quality estimate of the direction and intensity of these fluxes. Indeed, an element diffusion results in a depletion at its starting point and an enrichment at its endpoint. Figure 9 shows how this analysis is performed: the EDS maps of Cu, Au and Sn obtained at 240°C are subtracted from those obtained at 230°C during the first temperature increase (Fig. 5a, between 3 min 30 and 5 min). The chosen colour map makes it possible to visualize the parts that are enriched or depleted for a given element: the white colour indicates no change in composition. A concentration increase is in red and a concentration decrease in blue (in the online figure). Figure 9d shows the difference in mol.% of Cu, Au and Sn between 230 and 240°C over the entire element map (black line in Fig. 9a). To fully understand this, it must be borne in mind that the total thickness of the reactive zone increases as annealing proceeds, from 3.8 µm at 230°C (Table I) to 4.7 µm at 240°C (Table II).

At the Cu/Au interface, the voids are all formed between 230 and 240°C, and the surface area occupied by the voids increases and reaches a maximum at the end of the first temperature increase to 240°C (Fig. 5). As mentioned before, Au_3Cu is believed to disappear quickly and the phase sequence could be Cu/phase B/(Au,Cu)Sn during the growth of phase B. The formation of Kirkendall voids would, therefore, be related to the growth of phase B. Phase B growth is

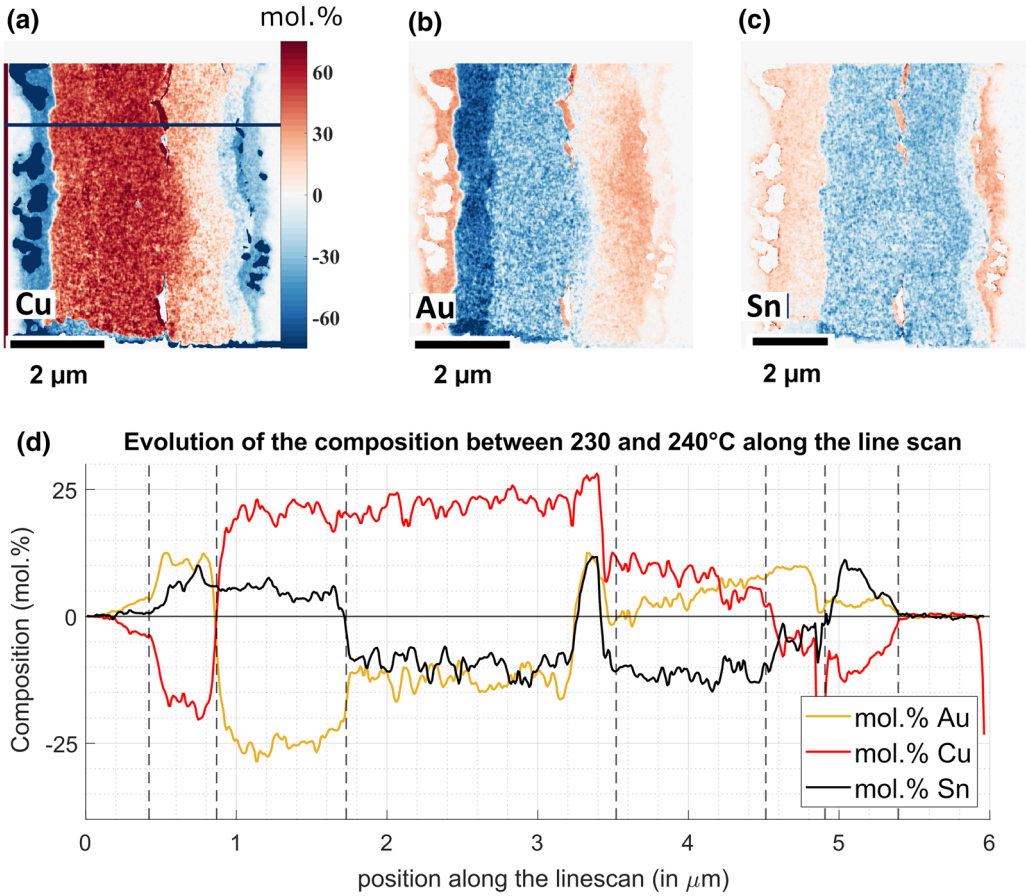

Fig. 9 Maps of (a) Cu, (b) Au and (c) Sn obtained by subtracting the EDS maps of each atom, measured at 240°C and 230°C. Colour code: no change in composition in white, concentration increase in red and concentration decrease in blue. The three images share the same colour bar (in mol.%). The differences in mole fractions of Cu, Au and Sn between 230 and 240°C along the black horizontal line (a) are shown in (d). The vertical dashed lines delineate areas with a homogeneous change in chemical composition (Color figure online).

only possible through Sn and Au enrichment at the interface with Cu and through Cu enrichment at the interface with (Au,Cu)Sn. These diffusion fluxes occur in opposite directions, i.e. the Cu flux from the Cu side to the B/(Au,Cu)Sn interface and the Sn and Au fluxes from the B/(Au,Cu)Sn interface to the Cu side. Figure 9 seems to confirm this mechanism with the presence of a Cu-depleted layer in phase B on the left side (Figs. 9a and d between 0.6 and 1 µm). This layer is in the former Cu substrate where phase B developed and, logically, was depleted in Cu and enriched in Au and Sn. Interestingly, the voids are found within this layer at the Cu/phase B interface. We can deduce that the Cu flux is greater than the Sn and Au fluxes, with a difference offset by a large flux of vacancies required to form these voids. It is an interesting result for Au-Cu-Sn systems since this has not been mentioned in any previous study.

At the Sn/Cu interface, void formation occurs in two steps and at two distinct interfaces (bottom white rectangles before and after 5 min in Fig. 5d). The first nucleation/growth of voids occurs at the $(Cu,Au)_6Sn_5/Cu_3Sn$ interface from 230 to 240°C, and the second at the reactive zone/Cu interface at about 240°C (Holding at 240°C section). EDS analysis, performed when the sample returns to room temperature, shows that the first voids, formed between 230 and 240°C, are located at the phase B/Cu_3Sn interface. The Cu_3Sn, the thickness of which remains constant during the temperature increase, probably has little involvement in the reactions. Therefore, it can be assumed that the voids are formed when $(Cu,Au)_6Sn_5$ transforms into phase B (Fig. 4a, Table II). This transformation is only possible through Cu and Au enrichment and Sn depletion (Fig. 8), as confirmed by the variations in the composition of the three elements during annealing (Fig. 9). Figure 9 can help to deduce the main direction of the diffusion fluxes: two Cu fluxes, the main one coming from the left and the other one crossing the Cu_3Sn layer, an Au flux coming from the left (blue to orange, Fig. 9b) and an Sn flux that seems to be mainly directed from right to left (strong Sn enrichment on the left, Fig. 9c). Sn is known to diffuse faster than Cu in Cu_6Sn_5.[34] This difference could explain the formation of Kirkendall voids. However, it is impossible to propose a precise mechanism to explain the formation of these voids without intermediate measurements.

Holding at 240°C

Within a short holding time, less than 1 min at 240°C, Cu_3Sn transforms into phase B on the Sn-rich side and $AuCu_3$ nucleates at the interface between Cu and phase B on the Au-rich side. The resulting microstructure can be described by the dark blue diffusion path, suggesting that all the interfaces are at equilibrium. The mean joint composition (down-pointing triangle in Fig. 8) is in the $AuCu_3$-phase B region in the phase diagram. It explains why Cu_3Sn practically disappears and $AuCu_3$ forms. The transformation of Cu_3Sn into phase B leads to the second stage of Kirkendall void nucleation at 240°C on the Sn-rich side, as mentioned previously (bottom white rectangle in Fig. 5d at about 5 min). At the end of the ramp to 240°C, the first voids are embedded within phase B (white arrow in the Sn map, Fig. 4a), exactly where the neighbouring Cu_3Sn phase has just been consumed. Kirkendall void growth continues during the first few minutes of holding at 240°C (top white rectangle in Fig. 5d at about 7–8 min). The movement of the voids to the right (Sect. Apparent Movement of the Voids at Both Interfaces) is probably due to a dominant Cu flux from the right side (as the vacancy flux is in the opposite direction to the net atom flux).

Over a longer annealing time of between 11 and 131 min, Cu_3Sn completely disappears, $AuCu_3$ also nucleates at the initially Sn-rich side (confirmed by the EDS for 11 min at 240°C), and the microstructure becomes Cu/$AuCu_3$/phase B/$AuCu_3$/Cu. Once again, all the interfaces are at equilibrium. Since the mean composition of the joint is in the phase B/$AuCu_3$ binary domain (regular pentagon in Fig. 8), the disappearance of Cu_3Sn is expected. Because of the thermodynamic driving force, the atoms of the former Cu_3Sn phase should react to increase the amount of the more stable phases ($AuCu_3$ and Phase B).

The Kirkendall voids formed earlier in the transformation influence the growth of $AuCu_3$ at the end of the diffusion process. On the Au-rich side the voids are spaced apart, allowing the reactive diffusion of atoms. In contrast, on the Sn-rich side, the voids cover a more significant part of the diffusion surface area and act as a diffusion barrier, which may explain the later formation of $AuCu_3$ (Fig. 5).

After 131 min at 240°C, the average composition of the joint is in the $AuCu_3$phase B/Cu_3Sn three-phase region (grey star, Fig. 8). One would expect Cu_3Sn to nucleate again for longer times.

In the Au-rich side, the formation and growth of $AuCu_3$ at the Cu / phase B interface induces a decrease in the size of the voids and even causes them to disappear, as shown clearly in Fig. 7c and d. The chemical reaction forming $AuCu_3$ from phase B and Cu implies that Au in phase B reacts with Cu. Au diffuses into $AuCu_3$ towards the Cu/$AuCu_3$ interface when $AuCu_3$ forms a continuous layer. The Cu atoms continue to diffuse through $AuCu_3$ in the opposite direction and may react with phase B to form $AuCu_3$ or diffuse further into the joint. A higher diffusion flux of Au than of Cu in $AuCu_3$ could explain the gradual disappearance of the voids. If phase B reacts with Cu to forms $AuCu_3$, the Sn released may be included in the B-phase lattice, which appears to be undersaturated in Sn in our experiments (its Sn composition is lower than in previous measurements, see Fig. 8).

Starting later, the process is similar in the Sn-rich side. The morphology of the voids is different; however, they now form a continuous layer that acts as a diffusion barrier. Consequently, diffusion can only take place in a reduced area that is free of voids (Fig. 4c). This area tends to expand as the voids are gradually filled (Figs. 4d and 7d). A closer examination of the sample after 11 min of heating shows that the Sn-rich side comprises three vertical voids: a thin one in the middle and two thicker ones at the top and bottom of the sample (Fig. 4c). Diffusion only occurs around the thin void in the middle, which is filled by $AuCu_3$ after 2 h at 240°C (Fig. 4d).

Conclusion

The mechanisms of reactive diffusion and Kirkendall void formation were investigated in the Cu-Au-Sn-Cu sandwich system. The experiments were conducted *in situ* in a transmission electron microscope.

A progressive enrichment in Cu induces the transformation of the Cu/Au/Sn/Cu diffusion couple during heating and holding at 240°C. For the present system, the evolution is as follows:

- After the bulk has been heated to 230°C, the phase sequence is only composed of binary compounds: Cu/Au_3Cu/(Au, Cu)Sn/(Cu, Au)$_6Sn_5$/Cu_3Sn/Cu. The diffusion paths in the Au-Cu-Sn ternary diagram show that the phase interfaces are in local thermodynamic equilibrium on the Sn-rich side and out of local thermodynamic equilibrium on the Au-rich side (both phases and interfaces).
- During heating from 230°C to 240°C, the ternary phase B forms and the phase sequence becomes Cu/phase B/Cu_3Sn/Cu. Only the Cu/Phase B interface is not in equilibrium.
- When the temperature is maintained at 240°C, the phase sequence becomes Cu/$AuCu_3$/phase B/Cu, then Cu/$AuCu_3$/phase B/$AuCu_3$/Cu. The phase interfaces of the latter sequence are at local thermodynamic equilibrium.
- As Cu enrichment continues, Cu_3Sn becomes stable for longer annealing times according to the thermodynamic equilibrium diagram. Cu_3Sn is then expected to nucleate again.

Nucleation and growth of Kirkendall voids were observed in parallel with reactive diffusion at both interfaces and can be explained by different mechanisms:

- On the Au-rich side, Kirkendall void formation seems to be related to phase B growth and is characterized by a few large equiaxed voids.
- On the Sn-rich side, void formation occurs in two steps at two interfaces. The first nucleation/growth of voids occurs at the (Cu, Au)$_6Sn_5$/Cu_3Sn interface from 230 to 240°C and seems to be related to phase B growth from (Cu, Au)$_6Sn_5$. The second nucleation/growth of voids occurs at the reactive zone/Cu interface at about 240°C and seems to be related to the phase B growth consecutive to the disappearance of the Cu_3Sn. In both steps, many small voids appear and merge together to form a continuous line of voids.
- Later in the heat treatment process, $AuCu_3$ formation on both sides induces a decrease in the size of the voids and even causes them to disappear.

Since the present work is devoted mainly to the formation and evolution of Kirkendall voids, some questions remain about the phase evolution in the joint, especially as a function of the initial Au and Sn content. This is part of a work in progress.

Supplementary Information The online version contains supplementary material available at https://doi.org/10.1007/s11664-021-09390-w.

Acknowledgments This work was carried out within the MATMECA consortium and supported by the ANR under contract number ANR-10-EQPX-37. It has benefited from the facilities of the MSSMat Laboratory, CNRS, CentraleSupélec, Université Paris-Saclay, France. The author would like to acknowledge the financial support from the DGA through a RAPID grant, and Bernard Ledain who has carried out the project. This work has also been possible thanks to all Meredit members, and especially Rémi Salmon who has overseen sample preparation. The authors are extremely grateful to the staff of CentraleSupélec (N. Ruscassier, M. Charters, P. Haghi-Ashtiani) for their valuable assistance. They extend their thanks to H.Q. Dong for the Au-Cu-Sn phase diagram assessed at 240°C.

Conflict of interest On behalf of all the authors, the corresponding author states that there is no conflict of interest.

References

1. B. Ledain, S. Secher, P. Kertsez, Method for producing interconnection in a multilayer printed circuits, US 2004/0060173 A1 (April 2004)
2. H. Dong, V. Vuorinen, T. Laurila, and M. Paulasto-Kröckel, Microstructural evolution and mechanical properties in (AuSn) Eut-Cu interconnections. *J. Electron. Mater.* 45, 5478 (2016).
3. H. Etschmaier, J. Novák, H. Eder, and P. Hadley, Reaction dynamics of diffusion soldering with the eutectic Au–Sn Alloy on copper and silver substrates. *Intermetallics* 20, 87 (2012).
4. Y.-W. Yen, C.-C. Jao, H.-M. Hsiao, C.-Y. Lin, and C. Lee, Investigation of the phase equilibria of Sn-Cu-Au Ternary and Ag-Sn-Cu-Au quaternary systems and interfacial reactions in Sn-Cu/Au couples. *J. Electron. Mater.* 36, 147 (2007).
5. S. Santra, S. Islam, R. Ravi, V. Vuorinen, T. Laurila, and A. Paul, Phase evolution in the AuCu/Sn system by solid-state reactive diffusion. *J. Electron. Mater.* 43, 3357 (2014).
6. C.H. Lin, C.Y. Yeh, and Y.W. Yen (2018) *Interfacial reactions between Sn and Au-XCu allo ys*, in *2018 International Conference on Electronics Packaging and IMAPS All Asia Conference (ICEP-IAAC)* (IEEE, Mie, Japan, 2018), pp. 59–64

7. C. Du, R. Soler, B. Völker, K. Matoy, J. Zechner, G. Langer, M. Reisinger, J. Todt, C. Kirchlechner, and G. Dehm, Au–Sn Solders Applied in Transient Liquid Phase Bonding: Microstructure and Mechanical Behavior. *Materialia* 8, 100503 (2019).
8. J.Y. Tsai, C.W. Chang, C.E. Ho, Y.L. Lin, and C.R. Kao, Microstructure Evolution of Gold-Tin Eutectic Solder on Cu and Ni Substrates. *J. Electron. Mater.* 35, 65 (2006).
9. C. Yang, and S. Chen, Interfacial Reactions in Au/Sn/Cu Sandwich Specimens. *Intermetallics* 18, 672 (2010).
10. J. Peng, H.S. Liu, H.B. Ma, X.M. Shi, and R.C. Wang, Microstructure Evolution and Mechanical Reliability of Cu/Au–Sn/Cu Joints During Transient Liquid Phase Bonding. *J. Mater. Sci.* 53, 9287 (2018).
11. H.Q. Dong, V. Vuorinen, X.M. Tao, T. Laurila, and M. Paulasto-Kröckel, Thermodynamic Reassessment of Au–Cu–Sn Ternary System. *J. Alloys Compd.* 588, 449 (2014).
12. O.B. Karlsen, A. Kjekshus, C. Romming, and E. Rost, The crystal structure of the low temperature $Au_{80-v}Cu_vSn_{20}$ Phase. *Acta. Chem. Scand.* 46, 1076 (1992).
13. D. Kim, J. Chang, J. Park, J.J. Pak (2011) Formation and behavior of Kirkendall voids within intermetallic layers of solder joints, J. Mater. Sci., 14
14. M.R. Pinnel, Diffusion-related behaviour of gold in thin film systems. *Gold Bull.* 12, 62 (1979).
15. M.R. Pinne, and J.E. Bennett, On the formation of the ordered phases CuAu and Cu3Au at a copper/gold planar interface. *Metall Trans A* 10, 741 (1979).
16. J. Yu, and J.Y. Kim, Effects of residual S on Kirkendall void formation at Cu/Sn–3.5Ag solder joints. *Acta Mater.* 56, 5514 (2008).
17. J.Y. Kim, and J. Yu, Effects of residual impurities in electroplated Cu on the Kirkendall void formation during soldering. *Appl. Phys. Lett.* 92, 092109 (2008).
18. L. Yin, and P. Borgesen, On the root cause of Kirkendall voiding in Cu_3Sn. *J. Mater. Res.* 26, 455 (2011).
19. G. Ross, V. Vuorinen, and M. Paulasto-Kröckel, Void formation and its impact on CuSn intermetallic compound formation. *J. Alloys Compd.* 677, 127 (2016).
20. K. Zeng, R. Stierman, T.-C. Chiu, D. Edwards, K. Ano, and K.N. Tu, Kirkendall void formation in eutectic SnPb solder joints on bare Cu and its effect on joint reliability. *J. Appl. Phys.* 97, 024508 (2005).
21. J.Y. Kim, Y.C. Sohn, and J. Yu, Effect of Cu content on the mechanical reliability of Ni/Sn–3.5Ag System. *J. Mater. Res.* 22, 770 (2007).
22. K. Cheng, H. Xu, B. Ma, J. Zhou, S. Tang, Y. Liu, C. Sun, N. Wang, M. Wang, L. Zhang, and Y. Du, An In-Situ study on the diffusion growth of intermetallic compounds in the Al–Mg diffusion couple. *J. Alloys Compd.* 810, 151878 (2019).
23. K. Cheng, J. Sun, H. Xu, J. Wang, C. Zhan, R. Ghomashchi, J. Zhou, S. Tang, L. Zhang, and Y. Du, Diffusion growth of \phi ternary intermetallic compound in the Mg-Al-Zn alloy system: in-situ observation and modeling. *J. Mater. Sci. Technol.* 60, 222 (2021).
24. J.M. Pauls, C.E. Shuck, A. Genç, S. Rouvimov, and A.S. Mukasyan, In-Situ transmission electron microscopy determination of solid-state diffusion in the aluminium–nickel system. *J. Solid State Chem.* 276, 114 (2019).
25. P.G. Kotula, and S.V. Prasad, Visualization of Kirkendall voids at Cu-Au interfaces by *in situ* TEM heating studies. *JOM* 71, 3521 (2019).
26. C.A. Schneider, W.S. Rasband, and K.W. Eliceiri, NIH image to imageJ: 25 years of image analysis. *Nat. Methods* 9, 671 (2012).
27. K. Eliceiri (2017) *ImageJ2: ImageJ for the next Generation of Scientific Image Data*, 26
28. J.B. Clark, Convention for plotting the diffusion paths in multiphase ternary diffusion couples on the isothermal section of a ternary phase diagram. *Trans. Met. Soc. AIME* 227, 1250 (1963).
29. J.S. Kirkaldy, and L.C. Brown, Diffusion behaviour in ternary, multiphase systems. *Can. Metall. Q.* 2, 89 (1963).
30. S. Prasad, and A. Paul, Growth and consumption rates of the phase layers during interdiffusion in a diffusion couple with finite end member. *J. Mater. Sci. Mater. Electron.* 23, 75 (2012).
31. U. Gösele, and K.N. Tu, Growth kinetics of planar binary diffusion couples: ''thin-film case'' versus ''bulk cases''. *J Appl Phys* 53, 10 (1982).
32. O.B. Karlsen, A. Kjekshus, and E. Rost, The ternary system Au-Cu-Sn. *Acta Chem. Scand*. 46, 147 (1992).
33. O.B. Karlsen, A. Kjekshus, and E. Rost, Ternary phases in the system Au-Cu-Sn. *Acta Chem. Scand* 44, 197 (1990).
34. A. Paul, C. Ghosh, and W.J. Boettinger, Diffusion parameters and growth mechanism of phases in the Cu-Sn System. *Metall. Mater. Trans. A* 42, 952 (2011).